Interactive impacts of fire and vegetation dynamics on global carbon and water budget using Community Land Model version 4.5

Hocheol Seo[1], and Yeonjoo Kim[1]

[1]Department of Civil and Environmental Engineering, Yonsei University, Seoul 03722, Korea.
Correspondence to: Yeonjoo Kim (yeonjoo.kim@yonsei.ac.kr)

Abstract

Fire plays an important role in terrestrial ecosystems. The burning of biomass affects carbon and water fluxes and vegetation distribution. To understand the effect of interactive processes of fire and ecological succession on surface carbon and water fluxes, this study employed the Community Land Model version 4.5 to conduct a series of experiments that included and excluded fire and dynamic vegetation processes. Results of the experiments that excluded the vegetation dynamics showed a global increase in net ecosystem production (NEP) in post-fire regions, whereas the inclusion of vegetation dynamics revealed a fire-induced decrease in NEP in some regions, which was depicted when the dominant vegetation type was changed from trees to grass. Carbon emissions from fires are enhanced by reduction in NEP when vegetation dynamics are considered; however, this effect is somewhat mitigated by the increase in NEP when vegetation dynamics are not considered. Fire-induced changes in vegetation modify the soil moisture profile because grasslands are more dominant in post-fire regions. This results in less moisture within the top soil layer than that in unburned regions, even though transpiration is reduced overall. These findings are different from those of previous fire model evaluations that ignored vegetation dynamics and thus, highlight the importance of interactive processes between fires and vegetation dynamics in evaluating recent model developments.

Keywords

Fire model, Dynamic vegetation model, Terrestrial carbon balance, Community Land Model, Terrestrial water balance

1 Introduction

Wildfire is a natural process that influences ecosystems and the global carbon and water cycle (Gorham, 1991; Bowman et al., 2009; Harrison et al., 2010). Climate and vegetation control the occurrence of fires and their spread, which in turn affects climate and vegetation (Vilà et al., 2001; Balch et al., 2008). When fire destroys forests and grasslands, the distribution of vegetation is also affected (Clement and Touffet, 1990; Rull, 1999). Wildfires are major sources of trace gases and aerosols, which are important elements in the radiative balance of the atmosphere (Scholes et al., 1996; Fiebig et al., 2003). Aerosols affect surface air temperature, precipitation, and circulation (Tarasova et al., 1999; Lau and Kim, 2006; Andreae and Rosenfeld, 2008).

Changes in soil properties occur in regions affected by fire; leaves and roots can be annihilated in those regions (Noble et al., 1980; Swezy and Agee, 1991). Each year, fires transport approximately 2.1 Pg of carbon from soil and vegetation into the atmosphere in the form of carbon dioxide and other carbon compounds (van der Werf et al., 2010). Harden et al. (2000) report that approximately 10–30% of annual net primary productivity (NPP) disappears through fires in upland forests. Transpiration and canopy evaporation decrease with the reduction in leaf numbers (Clinton et al., 2011; Beringer et al., 2015). Soil develops a water-repellent layer during fires due to intense heating (DeBano, 1991) and ash produced by biomass combustion impacts the quality of runoff (Townsend and Douglas, 2000).

In post-fire regions, plant distribution gradually changes over time from bare ground to grassland, shrubland, and finally to forest during ecological succession (Prach and Pyšek, 2001). Therefore, the structure and distribution of vegetation can be altered by fires in post-fire regions (Wardle et al., 1997). The existence of grass and trees in the savanna can be attributed to fires (Hochberg et al., 1994; Sankaran et al., 2004; Baudena et al., 2010). However, fires can also wipe out succession.

Fire affects many aspects of the Earth system. Therefore, a process-based representation of fires is included in dynamic global vegetation models (DGVMs), land surface models (LSMs), and Earth system models (ESMs; Rabin et al., 2017). Previous studies reported the incorporation of fire models into global climate models to investigate the occurrence and spread of fires and how they impact climate and vegetation (e.g., Pechony and Shindell, 2010; Li et al., 2012; 2013). Bond et al. (2005) used the Sheffield DGVM and performed the first global study on the extent to which fires determine global vegetation patterns by preventing ecosystems from achieving potential height, biomass, and dominant functional types expected under ambient conditions (i.e., potential vegetation).

In recent years, global fire models have become more complex (Hantson et al., 2016). Different fire models parameterize different impact factors such as fuel moisture, fuel size, probability of lightning, and human effects. In this respect, the Fire Model Intercomparison Project (FireMIP) evaluates the strength and weakness of each fire model by comparing the performance of different fire models and suggesting improvements for individual models (Rabin et al., 2017).

A process-based fire parameterization of intermediate complexity has been developed and assessed within the framework of the National Center for Atmospheric Research (NCAR) the Community Earth System Model (CESM) (Li et al. 2012; 2013; 2015). The satellite-based Global Fire Emission Database version 3 (GFED3), which is derived from the Moderate Resolution Imaging Spectroradiometer (MODIS) fire count products and the burned

61   area, has been used to improve fire parameterization. The impact of fires on carbon, water, and energy balance has

62   also been investigated within the CESM framework (Li et al., 2014; Li and Lawrence, 2017). However, although these

63   studies have considered land–atmosphere interactions using the Community Land Model (CLM) coupled with an

64   atmospheric model, they have ignored the changes in global vegetation patterns caused by fires, even though the initial

65   model developed by Li et al. (2012) was designed to consider the vegetation dynamics (i.e., changes in vegetation

66   distribution) within the CLM-DGVM.

67   It is important to understand the individual and combined impacts of fires and vegetation distribution on

68   water and carbon exchange; however, few studies to date have assessed these complicated global processes. Therefore,

69   in this study, we aim to understand the interactive effects of fires and ecological succession on carbon and water fluxes

70   on the land surface. Specifically, using the NCAR CLM, we conduct a series of numerical experiments that include

71   and exclude fire and dynamic vegetation processes. Our results show that the impact of fires on carbon and water

72   balance (especially in net ecosystem production (NEP) and soil moisture) on ecological succession is different from

73   that on static vegetation.

74   **2 Model and experimental design**

75   **2.1 Model description**

76   This study used CLM version 4.5, which is the land model of the NCAR CESM version 1.2. The CESM is

77   maintained by NCAR's Climate Global Dynamics Laboratory (CGD) and comprises different components such as

78   land, atmosphere, ocean, land ice, and ocean ice (Worley at el., 2011; Kay et al., 2012). Each component utilizes

79   various formulae to represent the complex interplay of physical, chemical, and biological processes and each can be

80   used either independently or as coupled (Smith et al., 2010; Neale et al., 2012; Bonan et al., 2013). Land surface in

81   the CLM is represented by sub-grid land cover (glacier, lake, wetland, urban, or vegetated) and vegetation coverage

82   is represented by 17 plant functional types (PFTs) comprising 11 tree PFTs, 2 crop PFTs, 3 grass PFTs, and bare

83   ground. For a detailed description of the model, please refer to Lawrence et al. (2011).

84   CLM can be run by including different levels of vegetation processes. In the satellite phenology (SP) option,

85   vegetation coverage of different PFTs is prescribed using satellite-based land cover data (Lawrence and Chase, 2007),

86   derived from a variety of satellite products including MODIS and Advanced Very High-Resolution Radiometer data.

87   Land fractions are divided into bare ground, grass, shrub, and evergreen/deciduous trees. In addition, grass, shrub, and

88   tree PFTs are classified into tropical, temperate, and boreal types, based on the physiology and climate rules of Nemani

89   et al. (1996). Vegetation is further divided into C3 or C4 plants based on MODIS-derived LAI values and the mapping

90   methods of Still et al. (2003). Crop is also prescribed based on the merged dataset of the MODIS-derived land cover

91   product and the global land cover in 2000 (GLC2000) (Ramankutty et al., 2008). Furthermore, the vegetation state

92   (i.e., leaf area index, LAI) of different PFTs on land surface can be set based on the satellite-derived climatological

93   data (Lawrence and Chase, 2007), which differ between months but not between years.

94   In addition to the SP option, CLM 4.5 can be extended using the biogeochemistry model (BGC) and dynamic

95   vegetation model (DV); CLM simulations with BGC without DV (BGConly) and BGC with DV (BGC-DV) can be

96   configured. BGConly simulates the carbon and nitrogen cycles in addition to biophysics and hydrology in a given

97   distribution of vegetation PFTs (Paudel et al., 2016). In BGConly, phenological variations of LAI are simulated and

98   whole-plant mortality is assumed as an annual mortality rate of 2% without biogeographical changes of the vegetation

99   distribution. In contrast, BGC-DV simulates biogeographical changes in the natural vegetation distribution and

100   mortality as well as seasonal changes of LAI (Castillo et al., 2012; 2013). A PFT can occupy a region or degenerate

101   by competing with other PFTs, or they can coexist under various environmental factors, such as light, soil moisture,

102   temperature, and fire (Zeng, 2010; Song and Zeng, 2013). Plant mortality in BGC-DV is determined by heat stress,

103   fire, and growth efficiency (Rauscher et al., 2015). Note that BGC-DV does not simulate the crop PFTs, which is

104   included in BGConly, because it simulates the changes in the natural vegetation only.

105   In the fire model (Li et al., 2012, 2013; Bonan et al., 2013), fire types are divided into four groups: non-peat

106   fires outside cropland and tropical closed forests, agricultural fires, deforestation fires in tropical closed forests, and

107   peat fires. Fire counts are determined based on natural and artificial ignition, fuel availability, fuel combustibility, and

108   anthropogenic and unsuppressed natural fires related to socioeconomic conditions. The burned area is calculated by

109   multiplying the fire count by the average fire spread, which is considered to be driven by wind speed, PFT, fuel

110   wetness, and socioeconomic factors. In other words, the burning and spread of fire are related to the CLM input

111   parameters of climate and weather conditions, vegetation conditions, socioeconomic conditions, and population

112   density. After biomass and peat burning are calculated, trace gas and aerosol emissions as well as carbon emissions,

113   which are the byproducts of fires, are estimated.

114   Once the burned area is identified, impacts of the fire on vegetation mortality, peat burning, and carbon cycle,

115   can be addressed. The amount of carbon emitted from the fire (E) is calculated as follows:

116          $E = A \cdot C \cdot CC,$ (1)

117   where A is the burned area; C is a vector of elements including carbon density of the leaf stem and the root and transfer

118   and storage of carbon; CC is the corresponding combustion completeness factor vector.

119   Burned area also impacts the carbon and nitrogen pools of the vegetation, which are related to leaf, stem, and

120   root; fire changes the vegetation state (e.g., LAI) and vegetation height during the burning period in both BGConly

121   and BGC-DV runs. However, the number of individual PFTs does not change in BGConly, but decreases by biomass

122   burning in BGC-DV. In other words, individual plants are killed by fire only when the DV option is included in the

123   model. The number of PFTs killed by fire ($P_{distrub}$) is calculated using equation (2).

124          $P_{distrub} = \frac{A_b}{f A_g} P\, \xi,$ (2)

125   where P is the population density for each PFT, ξ is the whole-plant mortality factor for each PFT, A_g is the grid cell

126   area, A_b is the burned area of each PFT, and f is the fraction of coverage of each PFT. The whole-plant mortality, the

127   rate at which plants die completely by fire, is a calibrated PFT-dependent parameter, which is 0.1 for broadleaf

128   evergreen trees, 0.13 for needleleaf evergreen trees, 0.07 for deciduous trees, 0.15 for shrubs, and 0.2 for grass (Li et

129   al., 2012).

130   The terrestrial carbon balance is affected when biomass is burned. The net ecosystem exchange (NEE) can

131   be estimated using NEP (NEP=NPP–heterotrophic respiration (Rh)) and carbon loss due to biomass burning (C_{fe}).

132 $$NEE = -NEP + C_{fe}. \tag{3}$$

2.2 Experimental design

134 A series of global numerical experiments were conducted in this study using a spatial resolution of 1.9° longitude ×
135 2.5° latitude. Global climate data from the Climate Research Unit (CRU)-National Centers for Environmental
136 Prediction (NCEP) reanalysis were used for atmospheric driving forcing of CLM. Data from 1901 to 2000 included 6
137 h precipitation, air temperature, wind speed, specific humidity, longwave radiation, and shortwave radiation. Figure 1
138 and Table 1 summarizes the experimental process used in this study. The BGC run for the year of 1850 was initialized
139 with the PFT distribution from the Land Use Harmonization (LUH) transient dataset for 1850 to 2005 (Hurtt et al.,
140 2006 to simulate the year 1850 equilibrium state, used to initialize the 20th century transient run. In the transient run,
141 the amount of atmospheric carbon dioxide is increased since the onset of the Industrial Revolution in 1850 and the
142 composition of land cover and vegetation is changed with the LUH dataset of Hurtt et al. (2006) (Vitousek et al., 1997;
143 Pitman et al., 2004). The final surface conditions should represent those of the year 2000 after running the transient
144 simulation using the CLM-BGC model.

145 Using the simulated surface conditions for the year 2000, four different 200 yr equilibrium CLM simulations
146 (BGConly and BGC-DV simulations with and without the fire model) were conducted (Table 1). For BGConly runs,
147 a restart file from the transient run was used with and without the fire model (hereafter, BGConly-F and BGConly-
148 NF, respectively). Similarly, the BGC-DV runs were performed using the same restart file to simulate the equilibrium
149 vegetation in 200 yr offline BGC-DV runs both with and without the fire model (hereafter, BGC-DV-F and BGC-DV-
150 NF, respectively; Erfanian et al., 2016). In BGC-DV runs, the initial land surface state was bare ground with the
151 vegetation previously in the system being entirely removed while soil conditions were adjusted with a restart file from
152 the transient run (i.e., BGC run for the 20th century in Table 1) (Catillo et al., 2012; Raushcher et al., 2015; Qiu and
153 Liu, 2016; Wang et al., 2016). Therefore, the vegetation state is quickly stabilized for 200 years of the BGC-DV runs
154 since the runs restart from the spun-up soil carbon condition (i.e., after decomposition spin-up). Furthermore, the last
155 30 yr results of the 200 yr runs are analyzed to focus on the equilibrium states of both BGConly and BGC-DV runs.
156 While the fire model is optional when using CLM with BGC, it is always run when using CLM with BGC-DV. Hence,
157 the model was modified when conducting the BGC-DV-NF run and the burned area was set to zero to neglect any fire
158 incidences.

159 A comparison between the BGConly-F and BGConly-NF runs enables the isolation of the impact of fire on
160 land surface, regardless of DV. In addition, the impact of fires and the interactive impacts of fires and vegetation
161 distribution on the Earth system can be identified by comparing the BGC-DV-F and BGC-DV-NF runs. Note that this
162 study focuses on the impact of fires and vegetation dynamics on land carbon and water fluxes by forcing the CLM
163 with the CRU-NCEP climate data (1961–2000) without considering the land–atmosphere feedbacks. Simulations were
164 run for 200 years from the initial surface conditions of the year 2000 to derive equilibrium land surface conditions. In
165 addition, the average surface conditions of the last 30 years were compared with the simulation results.

3 Results and discussion

3.1 Burned area

In this section, we evaluate how the simulated burned areas differ between the runs with and without vegetation dynamics, i.e., BGC-DV-F and BGConly-F runs. On average, the BGC-DV-F and BGConly-F runs show burned areas of 320 and 487 Mha yr^{-1}, respectively. These results are similar to those of previous studies that applied CLM (i.e., Li et al., 2012; Li and Lawrence, 2017). The fire model of Li et al. (2012) was originally developed by comparing the BGC-DV-F-type CLM simulations and resulted in 322 Mha yr^{-1} for 1997–2004. The BGC-DV-F simulation, under the equilibrium condition driven by the 1961–2000 CRU-NCEP data in this study, estimates a similar burned area (320 Mha yr^{-1}) to that of Li et al. (2012). Li and Lawrence (2017) estimated the annual burned area as 489 Mha, which is similar to that of BGConly-F (487 Mha), using a BGC-F type simulation coupled with CAM.

In comparison to the burned area of BGConly-F, BGC-DV-F simulates a relatively small burned area because agricultural fires are excluded in BGC-DV-F and only natural vegetation is simulated (Castillo et al., 2012) as well as because fewer trees and thus fewer fuel, feed backed from fire, are simulated in BGC-DV-F than in BGConly-F. Furthermore, the spatial distribution of burned areas in Figure 2 shows that BGC-DV-F particularly underestimates the burned area in Africa and Oceania compared to BGConly-F. The differences in vegetation distribution between BGC-DV-F and BGConly-F in Figure 3, where PFTs, excluding two crop PFTs, are simplified into six vegetation groups (broadleaf evergreen trees, needleleaf evergreen trees, deciduous trees, shrubs, grasses, and bare ground) (Rauscher et al., 2015), may impact the size of the burned area. In BGC-DV-F (Figure 3a), evergreen and deciduous trees show limited growth whereas grass and bare ground are dominant in some regions such as southern Africa. Overall, BGC-DV-F simulates trees on 37.5% of the global land area while BGConly-F, which is derived from observations (Figure 3b), indicates that trees cover 41.46% of the global land area (Table 2). More trees provide increased fuel for the occurrence and spread of fires in BGConly-F than in BGC-DV-F, consistent with the larger burned area in BGConly-F than in BGC-DV-F.

We also compare the model estimates to the satellite-based observational datasets of GFED (van der Werf et al., 2010; Giglio et al., 2013; van der Werf et al., 2017) (Figure 3). Although the model simulations are not intended to reflect the reality, but rather to understand the model mechanisms under the equilibrium states under the 1961–2000 climate forcing, it is still valuable to assess the model results using the observations. Different versions of GFED datasets provided different sized burned areas: GFED3 (van der Werf et al., 2010), GFED4 (Giglio et al., 2013), and GFED4 with small fires, i.e., GFED4s (van der Werf et al., 2017) suggest the burned area of 371 Mha yr-1 for 1997–2009, 348 Mha yr-1 for 1997–2011 and 513 Mha yr-1 for 1997–2016, respectively. In comparison to the most recent data, i.e., GFED4s, both BGConly-F and BGC-DV-F runs, especially BGC-DV-F, underestimate the burned area. Possible reasons for this underestimation in BGC-DV-F include the exclusion of agricultural fires and relatively small tree-dominated land coverage. The initial model development with a BGC-DV-F type simulation (Li et al., 2012) was carried out in comparison to GFED3 (van der Werf et al., 2010) and BGC-DV-F estimated a burned area (320 Mha yr-1) similar to that of GFED3 (i.e., 371 Mha yr-1).

201 **3.2 Interactions between vegetation and fire processes**

202 The impact of fires on vegetation distribution is assessed by comparing BGC-DV-F and BGC-DV-NF simulations
203 (Table 2 and Figures 4 and 5). Figure 4 shows the vegetation distribution of BGC-DV-NF (Figure 4a) and BGC-DV-
204 F minus BGC-DV-NF (Figure 4b: Figure 4a minus Figure 3a). The plots clearly indicate large differences in vegetation
205 cover in areas of high fire frequency (i.e., South Africa, South America, western North America, India, and a portion
206 of China) (Table 2), whereas areas with relatively low fire occurrence (i.e., the Arctic and desert regions) show small
207 differences.

208 We estimated the fraction of burned areas, where fractions are grouped into four categories (>10%, 10–1%,
209 1–0.1% and, <0.1%) for each vegetation type, and investigated the relationship between vegetation distribution and
210 fire occurrence. Differences in the vegetation distribution between BGC-DV-F and BGC-DV-NF in Figure 5 illustrate
211 a nonlinear change in vegetation distribution in response to post-fire area. The changes are small in areas with minimal
212 fire occurrence or where the burned area fraction is small (0.1–1%). However, relatively large changes in vegetation
213 distribution occur when the burned area fraction exceeds 1%. Furthermore, there are large changes in the vegetation
214 distribution in areas with burned area fractions above 10%, including increases in bare ground, grass, and shrubs
215 (31.19, 52.28, and 7.91%, respectively) but decreases in deciduous, needleleaf evergreen, and broadleaf evergreen
216 trees (8.85, 79.22, and 91.17%, respectively).

217 In ecosystems, plants die in regions where fires occur and grass with rapid growth rates occupies those
218 regions. Therefore, fire increases the ratio of bare ground and grassland but reduces the number of trees. However,
219 there are no significant changes in the global fraction of shrubs and deciduous trees in the middle of the ecological
220 succession process with respect to the presence or absence of fires (Table 2). When a fire occurs in a region where
221 shrubs grow, the ratio of shrubland is diminished (e.g., in the middle of North America in Figure 4b), but fire increases
222 the ratio of shrubland in regions where trees grow (e.g., in the southwestern Asia in Figure 4b). Similarly, the number
223 of deciduous trees increases or decreases due to fires. Thus, the role of fires in areas of shrubland and deciduous trees
224 varies with the region and the actual vegetation distribution is a result of many factors including fire, climate,
225 topography, and soil conditions (He et al., 2007; Cimalová and Lososová, 2009).

226 **3.3 Fire impact on carbon balance**

227 The direct and indirect impacts of fires on carbon balance were investigated for static and dynamic vegetation cover
228 (Figure 6 and Table 3). The impact of fires in BGConly was estimated by calculating the difference between BGConly-
229 F and BGConly-NF, averaged over the final 30 years of each 200 yr simulation. Similarly, the impact of fires in BGC-
230 DV was estimated by calculating the difference between BGC-DV-F and BGC-DV-NF.

231 Carbon emissions from fires (direct impacts) are shown in Figure 6. The spatial distribution of the BGConly
232 and BGC-DV runs is similar, but average annual emissions are higher in BGConly (3.5 Pg) than in BGC-DV (3.0 Pg)
233 because trees are less dominant in BGC-DV than in BGConly, which causes a reduced fuel load.

234 Carbon emission estimates from both BGConly and BGC-DV simulations are relatively high; however, they
235 do fall within the range of previous findings. For example, 1997–2014 GFED4s data estimated annual direct carbon
236 emissions as 2.3 Pg. Mouillot et al. (2006) estimated annual carbon emissions as 3.0 Pg for the end of the 20th century

237 and the 20th century average as 2.5 Pg. Li et al. (2012) estimated the 20th century emissions as 3.5 Pg C yr^{-1} using the

238 CLM3-DGVM and Li et al. (2014) and Yue et al. (2015) both estimated the 20th century emissions as 1.9 Pg C yr^{-1}

239 using the CLM4.5 and ORCHIDE land surface models, respectively.

240   In addition to direct carbon emissions from fires, fire influences terrestrial carbon sinks by impacting

241 ecosystem processes (Figure 6). Fire increases the NEP in post-fire regions in BGConly simulations (i.e., difference

242 between BGConly-F and BGConly-NF, Figure 6a), which is consistent with the findings of the previous studies (Li

243 et al., 2014). The overall NEP increase is 2.5 Pg C yr^{-1} in this study, which is greater than the value of 1.9 Pg C yr^{-1}

244 calculated by Li et al. (2014). However, Li et al. (2014) performed a transient simulation from 1850 to 2004, whereas

245 the BGConly runs in our study were conducted following an equilibrium simulation using the year 2000 as the

246 reference year, which means that no fire exchanges are caused by land cover changes.

247   Simulations that ignore vegetation dynamics (i.e., the BGConly runs in this study; Li et al., 2014; Yue et al.,

248 2015) show a global fire-induced NEP increase when comparing fire-on and fire-off runs. However, a decrease in fire-

249 induced NEP is apparent in some regions in BGC-DV simulations (i.e., differences between BGC-DV-F and BGC-

250 DV-NF, Figure 6b).This carbon sink reduction occurs in regions where dominant PFTs change from broadleaf and

251 needleleaf evergreen trees to grass (Table 3 and Figure 6). Table 4 shows the correlation coefficients between percent

252 changes in vegetation types and changes in carbon fluxes (NEP, NPP, and R_h) for six different PFTs in each grid cell

253 and Figure 7 shows the broadleaf evergreen tree, needleleaf evergreen tree, and grass PFTs. NEP changes are strongly

254 linked to changes in dominant PFTs; for example, decreases in broadleaf evergreen and needleleaf evergreen trees

255 and increases in grass. Furthermore, the changes in NEP and PFTs are related to the changes in NPP and R_h to some

256 extent. Our results differ from those of previous studies that did not consider vegetation dynamics (e.g., Amiro et al.,

257 2010) because the inclusion of vegetation dynamics enables the model to capture NEP decreases in post-fire regions

258 at the beginning of the post fire-succession.

259   Since land use changes are not considered in this study, the overall impact of fires was estimated by the sum

260 of direct carbon emissions from fires and terrestrial carbon sinks, i.e., NEP (Eq. 3). Both simulations resulted in net

261 carbon sources in the post-fire regions, even though different processes were involved. Direct carbon emissions from

262 fires (C_{fe} in Eq. 3) were partly negated by the increased NEP in the BGConly runs, but they were enhanced by the

263 reduction of NEP in BGC-DV runs.

3.4 Fire impact on water balance

265 The impact of fires on water balance was examined by estimating the changes in runoff, evapotranspiration, and soil

266 moisture between cases with and without fire. The differences between BGConly-F and BGConly-NF were assessed

267 for the case without considering the vegetation dynamics and differences between BGC-DV-F and BGC-DV-NF for

268 the case considering the vegetation dynamics (Table 5 and Figure 8). Increases in runoff and decreases in

269 evapotranspiration (ET) were observed in post-fire regions to a different degree, which is consistent with the results

270 of the previous studies (Neary et al., 2005; Li and Lawrence, 2017). Our study used CLM as a standalone model

271 without coupling it with atmospheric or ice models, whereas Li and Lawrence (2017) examined the impact of fires on

272   global water budget using CLM-BGC coupled with the CAM and CICE models and showed that the impact of fires

273   on global annual precipitation was limited.

274   Li and Lawrence (2017) demonstrated that a reduction in vegetation canopy (LAI; Table 6) is a critical

275   pathway for fires that decrease ET. Fire events lower the leaf area, which decreases vegetation transpiration and

276   canopy evaporation; however, they also expose more of the soil to the air and sunlight, which increases soil

277   evaporation. Post-fire decreases in vegetation height (Table 6) can increase and decrease ET because the resulting

278   decrease in land surface roughness potentially reduces water and energy exchange and leads to higher leaf

279   temperatures and wind speeds. In this study, both BGConly and BGC-DV runs show that the vegetation canopy is the

280   main pathway leading to a decrease in ET, which is similar to the findings of Li and Lawrence (2017). In addition, an

281   examination of the changes in the vegetation composition in post-fire regions shows that the overall impact of those

282   changes in ET and runoff does not differ greatly when dynamic vegetation is employed in the model.

283   The results show that fire-induced vegetation changes (from trees to grass or bare ground) in BGC-DV lead

284   to a significant decrease in canopy transpiration and increase in soil evaporation relative to BGConly runs. Fire

285   destroys plant roots and leaves; changes in the dominant vegetation types in BGC-DV lead to changes in the soil

286   moisture profile through reduced transpiration (Figure 9 and Table 7). Consequently, there is less water stress in each

287   soil layer in the burned areas than in unburned areas. Grasslands dominate the post-fire regions in BGC-DV runs and

288   they absorb and transpire more water from the top soil layer than trees (Mazzacavallo and Kulmatiski, 2015).

289   Therefore, there is less moisture in the top soil layers in fire affected regions than in unburned regions, although the

290   overall transpiration is diminished. In summary, fire has an impact on vegetation distribution, which in turn impacts

291   the soil water profile.

292   Despite the differences in soil moisture and vegetation canopy and height, changes in ET and runoff do not

293   vary significantly between BGConly and BGC-DV. Thus, including dynamic vegetation does not impact the

294   physiological and physical processes of evapotranspiration and runoff, respectively. However, changes in ET and

295   runoff can be amplified in BGC-DV than in BGConly by modeling the land–atmosphere interactions with a coupled

296   land–atmosphere model (e.g., CLM–CAM) because changes in land characteristics in BGC-DV would feed back to

297   the changes in precipitation. Therefore, the limited impact of fires on precipitation in Li and Lawrence (2017) with

298   the coupled model would be increased by including dynamic vegetation in the model.

299   **4 Conclusions**

300   To understand the interplay between the vegetation dynamics and the impact of fires, we conducted a series of

301   numerical experiments using CLM with and without fires and dynamic vegetation. In particular, we investigated the

302   impact of fires on vegetation distribution and how these changes influence terrestrial carbon and water fluxes.

303   The results show that fire interrupts the process of ecological succession, which impacts the global vegetation

304   distribution. Fire transforms some regions into bare ground and grassland starts to quickly dominate those landscapes

305   because grass grows faster than trees. For shrubs and deciduous trees in the mid-stages of ecological succession, there

306   were no large differences in the overall coverage ratios between simulations that included vegetation dynamics and

307   those that did not. Simulations that did not consider vegetation dynamics showed a fire-induced global increase in

308   NEP; however, a fire-induced decrease in NEP was detected in some regions in BGC-DV runs. A carbon sink
309   reduction was also detected in regions where the dominant PFT changed from broadleaf and needleleaf evergreen
310   trees to grass. While carbon emissions from fires were partly negated by increased terrestrial carbon sinks (NEP) in
311   BGConly runs, they were enhanced by the reduction of terrestrial carbon sinks in BGC-DV runs when dynamic
312   vegetation was considered.

313   Fire-induced changes in vegetation from trees to grass or bare ground resulted in a decrease in canopy
314   transpiration and increased soil evaporation in post-fire regions in BGC-DV runs; however, there were no significant
315   differences in the overall impact on ET and runoff between the simulations that used dynamic vegetation and those
316   that did not. However, changes in dominant vegetation types in BGC-DV led to changes in the soil moisture profile.
317   Furthermore, the increased distribution of grassland cover was more dominant in post-fire regions, which then resulted
318   in less moisture in the top soil layers than in unburned areas, although transpiration diminished overall.

319   Enabling the vegetation dynamics module in the CLM improves the understanding of the interactive impacts
320   of fires and vegetation dynamics. However, uncertainty still exists because of the limitations in the simulations of
321   equilibrium vegetation distribution using CLM with BGC-DV-F; the final equilibrium vegetation state of the BGC-
322   DV model did not always correspond to the observed distribution (Figure 3). For example, shrubs in the tundra were
323   rare in both BGC-DV-F and BGC-DV-NF runs. Furthermore, crops, needleleaf evergreen boreal, and shrub boreal
324   cannot be simulated by the DV module, as also reported in previous studies (Zeng et al., 2008).

325   The fire module in CLM is parameterized to estimate the occurrence, spread, and impacts of fires. Thresholds
326   used to estimate fuel combustibility depend on relative humidity and surface air temperature; however, these values
327   may not be suitable for all regions (Zhang et al., 2016). In addition, the economic impact of fire occurrence and the
328   socioeconomic impact of fire spread are estimated using the input datasets of population density (person km^{-2}) and
329   GDP (US\$ per capita), respectively (Li et al., 2013). Uncertainty due to socioeconomic factors should be noted for
330   both historical and future simulations because changes in these factors may vary by country (Steelman and Burke,
331   2006). It is evident that our understanding of fires needs to improve because fires play an important role in the
332   distribution of vegetation and in carbon, water, and energy cycles. This study shows that fire models are strongly
333   impacted by vegetation distribution; therefore, fire simulations would improve with the advancement of dynamic
334   vegetation models.

335   **Code and Data Availability**

336   The code of and input datasets for CLM were downloaded from the NCAR CLM website (refer to cesm.ucar.edu).

337   **Author Contributions**

338   YK and HS designed the study and HS performed the model simulations by processing the data and modifying the
339   code. Both YK and HS analyzed the results and wrote the manuscript.

Acknowledgements

This study was supported by the Basic Science Research Program through the National Research Foundation of Korea, which was funded by the Ministry of Science, ICT & Future Planning (2018R1A1A3A04079419), and by the Korea Polar Research Institute (KOPRI, PN17900).

Conflict of Interest

The authors declare that they have no conflicts of interest.

References

Andreae, M. O., and Rosenfeld, D.: Aerosol-cloud-precipitation interactions. Part 1. The nature and sources of cloud-active aerosols, Earth Sci. Rev., 89(1–2), 13–41, doi.org/10.1016/j.earscirev.2008.03.001, 2008.

Amiro, B. D., Barr, A. G., Barr, J. G., Black, T. A., Bracho, R., Brown, M., Chen, J., Clark, K. L., Davis, K. J., Desai, A. R., Dore, S., Engel, V., Fuentes, J. D., Goldstein, A. H., Goulden, M. L., Kolb, T. E., Lavigne, M. B., Law, B. E., Margolis, H. A., Martin, T., McCaughey, J. H., Misson, L., Montes-Helu, M., Noormets, A., Randerson, J. T., Starr, G., and Xiao, J.: Ecosystem carbon dioxide fluxes after disturbance in forests of North America, J. Geophys. Res.-Biogeosci., 115(4), doi.org/10.1029/2010JG001390, 2010.

Balch, J. K., Nepstad, D. C., Brando, P. M., Curran, L. M., Portela, O., de Carvalho, O., and Lefebvre, P.: Negative fire feedback in a transitional forest of southeastern Amazonia, Global Change Biol., 14(10), 2276–2287, doi.org/10.1111/j.1365-2486.2008.01655.x, 2008.

Baudena, M., D'Andrea, F., and Provenzale, A.: An idealized model for tree-grass coexistence in savannas: The role of life stage structure and fire disturbances, J. Ecol., 98(1), 74–80, doi.org/10.1111/j.1365-2745.2009.01588.x, 2010.

Beringer, J., Hutley, L., Abramson, D., Arndt, S., Briggs, P., Bristow, M., Canadell, J., Cernusak, L., Eamus, D., Edwards, A., Evans, B., Fest, B., Goergen, K., Grover, S., Hacker, J., Haverd, V., Kanniah, K., Livesley, S., Lynch, A., Maier, S., Moore, C., Raupach, M., Russell-Smith, J., Scheiter, S., Tapper, N., and Uotila, P.: Fire in Australian savannas: From leaf to landscape, Global Change Biol., 21(1), 62–81, doi.org/10.1111/gcb.12686, 2015.

Bonan, G. B., Drewniak, B., Huang, M., Koven, C. D., Levis., S., Li, F., Riley, W. J., Subin, Z. M., Swenson, S. C. and Thronton, P. E.: Technical Description of Version 4.5 of the Community Land Model (CLM), NCAR/TN-486+STR, NCAR, Boulder, Colo., 2013.

Bond, W. J., Woodward, F. I., and Midgley, G. F.: The global distribution of ecosystems in a world without fire, New Phytol., 165(2), 525–538, doi.org/10.1111/j.1469-8137.2004.01252.x, 2005.

Bowman, D., Balch, J., Artaxo, P., Bond, W., Carlson, J., Cochrane, M., Antonio, C., Defries, R., Doyle, J., Harrison, S., Johnston, F., Keeley, J., Krawchuk, M., Kull, C., Marston, J., Moritz. M., Prentice,I., Roos, C., Scott, A., Swetnam, T., van der Werf, G., and Pyne, S.: Fire in the Earth System, Science, 324(5926), 481–484, doi.org/10.1126/science.1163886, 2009.

Castillo, C. K. G., and Gurney, K. R.: A sensitivity analysis of surface biophysical, carbon, and climate impacts of tropical deforestation rates in CCSM4-CNDV, J. Clim., 26(3), 805–821, doi.org/10.1175/JCLI-D-11-00382.1, 2013.

375 Castillo, C. K. G., Levis, S., and Thornton, P.: Evaluation of the new CNDV option of the community land model:

376 Effects of dynamic vegetation and interactive nitrogen on CLM4 means and variability, J. Clim., 25(11), 3702–3714,

377 doi.org/10.1175/JCLI-D-11-00372.1, 2012.

378 Cimalová, Š., and Lososová, Z.: Arable weed vegetation of the northeastern part of the Czech Republic: Effects of

379 environmental factors on species composition, Plant Ecol., 203(1), 45–57, doi.org/10.1007/s11258-008-9503-1, 2009.

380 Clement, B., and Touffet, J.: Plant Strategies and Secondary Succession on Brittany Heathlands after Severe Fire, J.

381 Veg. Sci., 1(2), 195–202, doi.org/10.2307/3235658, 1990.

382 Clinton, B. D., Maier, C. A., Ford, C. R., and Mitchell, R. J.: Transient changes in transpiration, and stem and soil

383 CO_2efflux in longleaf pine (Pinus palustris Mill.) following fire-induced leaf area reduction, Trees – Struct. Funct.,

384 25(6), 997–1007, doi.org/10.1007/s00468-011-0574-6, 2011.

385 DeBano, L.F.: The effects of fire on soil properties, United States Department of Agriculture Forestry Service General

386 Technical Report, INT-2, 151–156., 1991.

387 Erfanian, A., Wang, G., Yu, M., and Anyah, R.: Multimodel ensemble simulations of present and future climates over

388 West Africa: Impacts of vegetation dynamics, J. Adv. Model. Earth Syst., 8(3), 1411–1431,

389 doi.org/10.1002/2016MS000660, 2016.

390 Fiebig, M., Stohl, A., Wendisch, M., Eckhardt, S., and Petzold, A.: Dependence of solar radiative forcing of forest

391 fire aerosol on ageing and state of mixture, Atmos. Chem. Phys. Discuss., 3(2), 1273-1302, doi.org/10.5194/acp-3-

392 881-2003, 2003.

393 Giglio, L., Randerson, J. T., and van der Werf, G. R.: Analysis of daily, monthly, and annual burned area using the

394 fourth-generation global fire emissions database (GFED4), J. Geophys. Res.-Biogeo., 118(1), 317–328,

395 doi.org/10.1002/jgrg.20042, 2013.

396 Gorham, E.: Northern Peatlands : Role in the Carbon Cycle and Probable Responses to Climatic Warming, Ecol. Appl.,

397 1(2), 182–195, doi.org/10.2307/1941811, 1991.

398 Hantson, S., Arneth, A., Harrison, S. P., Kelley, D. I., Prentice, I. C., Rabin, S. S., Archibald, S., Mouillot, F., Arnold,

399 S. R., Artaxo, P., Bachelet, D., Ciais, P., Forrest, M., Friedlingstein, P., Hickler, T., Kaplan, J. O., Kloster, S., Knorr,

400 W., Lasslop, G., Li, F., Mangeon, S., Melton, J. R., Meyn, A., Sitch, S., Spessa, A., van der Werf, G. R., Voulgarakis,

401 A., and Yue, C.: The status and challenge of global fire modelling, Biogeosciences, 13(11), 3359–3375,

402 doi.org/10.5194/bg-13-3359-2016, 2016.

403 Harden, J. W., Trumbore, S. E., Stocks, B. J., Hirsch, A., Gower, S. T., O'Neill, K. P., and Kasischke, E. S.: The role

404 of fire in the boreal carbon budget, Global Change Biol., 6(Suppl. 1), 174–184, doi.org/10.1046/j.1365-

405 2486.2000.06019.x, 2000.

406 Harrison, S.P., Marlon, J.R. and Bartlein, P.J.: Fire in the Earth System, Changing climates, earth systems and society

407 (ed.by J. Dodson), 21–48, Springer, Dordrecht, 2010.

408 He, M. Z., Zheng, J. G., Li, X. R., and Qian, Y. L.: Environmental factors affecting vegetation composition in the

409 Alxa Plateau, China, J. Arid. Environ., 69(3), 473–489, doi.org/10.1016/j.jaridenv.2006.10.005, 2007.

410 Hochberg, M. E., Menaut, J. C., and Gignoux, J.: The Influences of Tree Biology and Fire in the Spatial Structure of

411 the West African Savannah, J. Ecol., 82(2), 217-226, doi.org/10.2307/2261290, 1994.

412 Hurtt, G. C., Frolking, S., Fearon, M. G., Moore, B., Shevliakova, E., Malyshev, S., Pacala, S., and Houghton, R.: The
413 underpinnings of land-use history: three centuries of global gridded land-use transitions, woodharvest activity, and
414 resulting secondary lands. Glob. Change Biol. 12, 1208-1229. doi.org/10.1111/j.1365-2486.2006.01150.x, 2006.

415 Kay, J. E., Hillman, B. R., Klein, S. A., Zhang, Y., Medeiros, B., Pincus, R., Gettelman, A., Eaton, B., Boyle, J.,
416 Marchand, R., and Ackerman, T. P.: Exposing global cloud biases in the Community Atmosphere Model (CAM) using
417 satellite observations and their corresponding instrument simulators, J. Clim., 25(15), 5190–5207,
418 doi.org/10.1175/JCLI-D-11-00469.1, 2012.

419 Lau, K. M., and Kim, K. M.: Observational relationships between aerosol and Asian monsoon rainfall, and circulation,
420 Geophys. Res. Lett., 33(21), L21810, doi.org/10.1029/2006GL027546, 2006.

421 Lawrence, D. M., Oleson, K. W., Flanner, M. G., Thornton, P. E., Swenson, S. C., Lawrence, P. J., Zeng, X., Yang,
422 Z., Levis, S., Sakaguchi, K., Bonan., G. B., and Slater, A. G.: Parameterization improvements and functional and
423 structural advances in Version 4 of the Community Land Model, J. Adv. Model. Earth Syst., 3(1),
424 doi.org/10.1029/2011MS00045, 2011.

425 Lawrence, P. J., and Chase, T. N.: Representing a new MODIS consistent land surface in the Community Land Model
426 (CLM 3.0), J. Geophys. Res.-Biogeo, 112(1), doi.org/10.1029/2006JG000168, 2007.

427 Li, F., and Lawrence, D. M.: Role of fire in the global land water budget during the twentieth century due to changing
428 ecosystems, J. Clim., 30(6), 1893–1908, doi.org/10.1175/JCLI-D-16-0460.1, 2017.

429 Li, F., Bond-Lamberty, B., and Levis, S.: Quantifying the role of fire in the Earth system - Part 2: Impact on the net
430 carbon balance of global terrestrial ecosystems for the 20th century, Biogeosciences, 11(5), 1345–1360,
431 doi.org/10.5194/bg-11-1345-2014, 2014.

432 Li, F., Levis, S., and Ward, D. S.: Quantifying the role of fire in the Earth system - Part 1: Improved global fire
433 modeling in the Community Earth System Model (CESM1), Biogeosciences, 10(4), 2293–2314, doi.org/10.5194/bg-
434 10-2293-2013, 2013.

435 Li, F., Zeng, X. D., and Levis, S.: A process-based fire parameterization of intermediate complexity in a dynamic
436 global vegetation model, Biogeosciences, 9(7), 2761–2780, doi.org/10.5194/bg-9-2761-2012, 2012.

437 Mazzacavallo, M. G., and Kulmatiski, A.: Modelling water uptake provides a new perspective on grass and tree
438 coexistence, PLoS ONE, 10(12), e0144300, doi.org/10.1371/journal.pone.0144300, 2015.

439 Mouillot, F., Narasimha, A., Balkanski, Y., Lamarque, J.-F., and F,eld, C. B.: Global carbon emissions from biomass
440 burning in the 20th century, Geophys. Res. Lett., 33(1), L01801, doi.org/10.1029/2005GL024707, 2006.

441 Neale, R. B., et al.: Description of the NCAR Community Atmosphere Model (CAM5.0), NCAR/TN-486+STR,
442 NCAR, Boulder, Colo., 2012.

443 Neary, D. G. ., Ryan, K. C., and DeBano, L. F.: Wildland Fire in Ecosystems, effects of fire on soil and water, General
444 Technical Report RMRS-GTR-42, 4. U.S. Department of Agriculture, Forest Service, Rocky Mountain Research
445 Station, Ogden, UT., 2005.

446 Nemani, R. R., Running, S. W., Pielke, R. a, and CHase, T. N.: Global vegetation cover changes from coarse resolution
447 satellite data, J. Geophys. Res.-Atmos., 101(D3), 7157–7162, doi.org/Doi 10.1029/95jd02138, 1996.

448 Noble, J. C., Smith, A. W. and Leslie, H. W.: Fire in the mallee shrublands of western New South Wales, Rangeland
449 J., 2(1), 104–114, 1980.

450 Paudel, R., Mahowald, N. M., Hess, P. G. M., Meng, L., and Riley, W. J.: Attribution of changes in global wetland
451 methane emissions from pre-industrial to present using Attribution of changes in global wetland methane emissions
452 from pre-industrial to present using CLM4.5-BGC, Environ. Res. Lett., 11(3), doi:10.1088/1748-9326/11/3/034020,
453 2016.

454 Pechony, O., and Shindell, D. T.: Driving forces of global wildfires over the past millennium and the forthcoming
455 century, PNAS, 107(45), 19167–19170, doi.org/10.1073/pnas.1003669107, 2010.

456 Pitman, A. J., Narisma, G. T., Pielke, R. A., and Holbrook, N. J.: Impact of land cover change on the climate of
457 southwest Western Australia, J. Geophys. Res.-Atmos., 109(D18), D18109, doi.org/10.1029/2003JD004347, 2004.

458 Prach, K., and Pyšek, P.: Using spontaneous succession for restoration of human-disturbed habitats: Experience from
459 Central Europe, Ecol. Eng., 17(1), 55–62, doi.org/10.1016/S0925-8574(00)00132-4, 2001.

460 Qiu, L., and Liu, X.: Sensitivity analysis of modelled responses of vegetation dynamics on the Tibetan Plateau to
461 doubled CO2 and associated climate change, Theor. Appl. Climatol., 124(1–2), 229–239, doi.org/10.1007/s00704-
462 015-1414-1, 2016.

463 Rabin, S. S., Melton, J. R., Lasslop, G., Bachelet, D., Forrest, M. ,Hantson, S., Kaplan, J. O., Li, F., Mangeon, S.,
464 Ward, D. S., Yue, C., Arora, V. K., Hickler, T. ,Kloster, S., Knorr, W., Nieradzik, L., Spessa, A., Folberth, G. A.,
465 Sheehan, T., Voulgarakis, A., Kelley, D. I., Colin Prentice, I., Sitch, S., Harrison, and S., Arneth, A.: The Fire
466 Modeling Intercomparison Project (FireMIP), phase 1: Experimental and analytical protocols with detailed model
467 descriptions, Geosci. Model Dev., 10, 1175-1197, doi.org/10.5194/gmd-10-1175-201, 2017.

468 Ramankutty, N., Evan, A., Monfreda, C., and Foley, J.: Farming the planet: 1. Geographic distribution of global
469 agricultural lands in the year 2000, Global Biogeochem. Cycles, 22, GB1003, doi:10.1029/2007GB002952, 2008.

470 Rauscher, S. A., Jiang, X., Steiner, A., Williams, A. P., Michael Cai, D., and McDowell, N. G.: Sea surface
471 temperature warming patterns and future vegetation change, J. Clim., 28(20), 7943–7961, doi.org/10.1175/JCLI-D-
472 14-00528.1, 2015.

473 Rull, V.: A palynological record of a secondary succession after fire in the Gran Sabana, Venezuela, J. Quat. Sci.,
474 14(2), 137–152, doi:10.1002/(SICI)1099-1417(199903)14:2<137::AID-JQS413>3.0.CO;2-3, 1999.

475 Sankaran, M., Ratnam, J., and Hanan, N. P.: Tree-grass coexstence in savannas revisited - Insights from an
476 examination of assumptions and mechanisms invoked in existing models, Ecol. Lett., 7(6), 480–490,
477 doi.org/10.1111/j.1461-0248.2004.00596.x, 2004.

478 Scholes, R. J., Ward, D. E., and Justice, C. O.: Emissions of trace gases and aerosol particles due to vegetation burning
479 in southern hemisphere Africa, J. Geophys. Res., 101(D19), 23,623-23,682, 1996.

480 Smith R, et al.: The Parallel Ocean Program (POP) reference manual: Ocean component of the Community Climate
481 System Model (CCSM), Technical Report LAUR-10-01853, Los Alamos National Laboratory, 2010.

482 Song, X., and Zeng, X.: Investigation of uncertainties of establishment schemes in dynamic global vegetation models,
483 Adv. Atmos. Sci., 31(1), 85–94, doi.org/10.1007/s00376-013-3031-1, 2014.

484   Steelman, T. A., and Burke, C. A.: Is wildfire policy in the United States sustainable?, J. Forest., 33, 67–72,
485   doi.org/10.2139/ssrn.1931057, 2007.

486   Still, C. J., Berry, J. A., Collatz, G. J., and DeFries, R. S.: Global distribution of C 3 and C 4 vegetation: Carbon cycle
487   implications, Global Biogeochem. Cycles, 17(1), 6-1-6–14, doi.org/10.1029/2001GB001807, 2003.

488   Swezy, D. M., and Agee, J. K.: Prescribed-fire effects on fine-root and tree mortality in old-growth ponderosa pine,
489   Can. J. For. Res., 21(5), 626–634, doi.org/10.1139/x91-086, 1991.

490   Tarasova, T. A., Nobre, C. A., Holben, B. N., Eck, T. F., and Setzer, A.: Assessment of smoke aerosol impact on
491   surface solar irradiance measured in the Rondônia region of Brazil during Smoke, Clouds, and Radiation – Brazil, J.
492   Geophys. Res.-Atmos., 104(D16), 19161–19170, doi.org/10.1029/1999JD900258, 1999.

493   Townsend, S., and Douglas, M. M.: The effect of three fire regimes on stream water quality, water yield and export
494   coefficients in a tropical savanna (Northern Australia), J. Hydrol., 229, 118–137, 2000.

495   van der Werf, G. R., Randerson, J. T., Giglio, L., Collatz, G. J., Mu, M., Kasibhatla, P. S., Morton, D. C., DeFries, R.
496   S., Jin, Y., and van Leeuwen, T. T.: Global fire emissions and the contribution of deforestation, savanna, forest,
497   agricultural, and peat fires (1997–2009), Atmos. Chem. Phys., 10, 11707–11735, 2010.

498   van der Werf, G. R., Randerson, J. T., Giglio, L., van Leeuwen, T. T., Chen, Y., Rogers, B. M., Mu, M., van Marle,
499   M. J. E., Morton, D. C., Collatz, G. J., Yokelson, R. J., and Kasibhatla, P. S.: Global fire emissions estimates during
500   1997–2016, Earth Syst. Sci. Data, 9, 697-720, doi.org/10.5194/essd-9-697-2017, 2017.

501   Vilà, M., Lloret, F., Ogheri, E., and Terradas, J.: Positive fire-grass feedback in Mediterranean Basin woodlands, For.
502   Ecol. Manage., 147, 3–14. 2001.

503   Vitousek, P. M., Mooney, H. a, Lubchenco, J., and Melillo, J. M.: Human Domination of Earth' s Ecosystems, Science,
504   277(5325), 494–499, doi.org/10.1126/science.277.5325.494, 1997.

505   Wang, G., Yu, M., Pal, J. S., Mei, R., Bonan, G. B., Levis, S., and Thornton, P. E.: On the development of a coupled
506   regional climate–vegetation model RCM–CLM–CN–DV and its validation in Tropical Africa, Clim. Dyn., 46(1–2),
507   515–539, doi.org/10.1007/s00382-015-2596-z, 2016.

508   Wardle, D., Olle, Z., Greger, H., and Gallet, C.: The Influence of Island Area on Ecosystem Properties The Influence
509   of Island Area on Ecosystem Properties, Science, 277(5330), 1296–1300, doi.org/10.1126/science.277.5330.1296,
510   1997.

511   Worley, P. H., Mirin, A. A., Craig, A. P., Taylor, M. A., Dennis, J. M., and Vertenstein, M.: Performance of the
512   community earth system model, in: High Performance Computing, Networking, Storage and Analysis (SC), 2011
513   International Conference, Seattle, WA, 2011.

514   Yue, C., Ciais, P., Cadule, P., Thonicke, K., and Van Leeuwen, T. T.: Modelling the role of fires in the terrestrial
515   carbon balance by incorporating SPITFIRE into the global vegetation model ORCHIDEE -Part 2: Carbon emissions
516   and the role of fires in the global carbon balance, Geosci. Model Dev., 8(5), 1321–1338, doi.org/10.5194/gmd-8-1321-
517   2015, 2015.

518   Zeng, X.: Evaluating the dependence of vegetation on climate in an improved dynamic global vegetation model, Adv.
519   Atmos. Sci., 27(5), 977–991, 2010.

520   Zeng, X., Zeng, X., and Barlage, M.: Growing temperate shrubs over arid and semiarid regions in the Community
521   Land Model-Dynamic Global Vegetation Model, Global Biogeochem. Cycles, 22(3), GB3003,
522   doi.org/10.1029/2007GB003014, 2008.
523   Zhang, L., Mao, J., Shi, X., Ricciuto, D., He, H., Thornton, P., Yu, G., Li, P., Liu, M., Ren, X., Han, S., Li, Y., Yan,
524   J., Hao, Y., and Wang, H.: Evaluation of the Community Land Model simulated carbon and water fluxes against
525   observations over ChinaFLUX sites, Agric. For. Meteorol., 226–227, 174–185,
526   doi.org/10.1016/j.agrformet.2016.05.018, 2016.
527
528
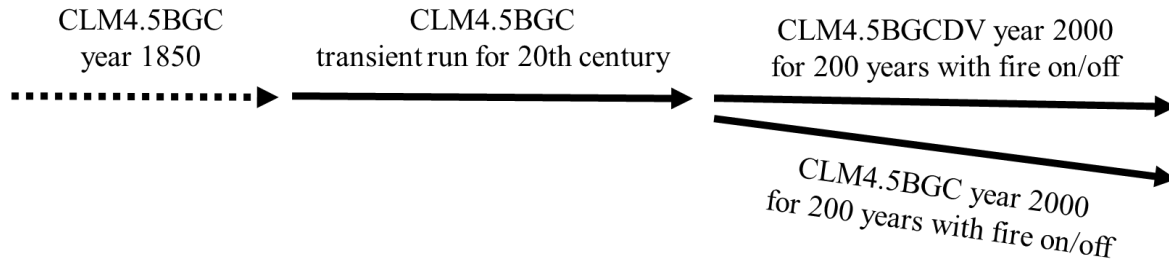
529

530

531 **Figure 1: Flowchart showing model simulations conducted to investigate the interactive impact of fires and ecological**
532 **succession on the Earth system using Community Land Model (CLM4.5) simulations extended with biogeochemistry**
533 **(CLM4.5BGC) and BGC with dynamic vegetation (CLM4.5BGCDV).**

534

535
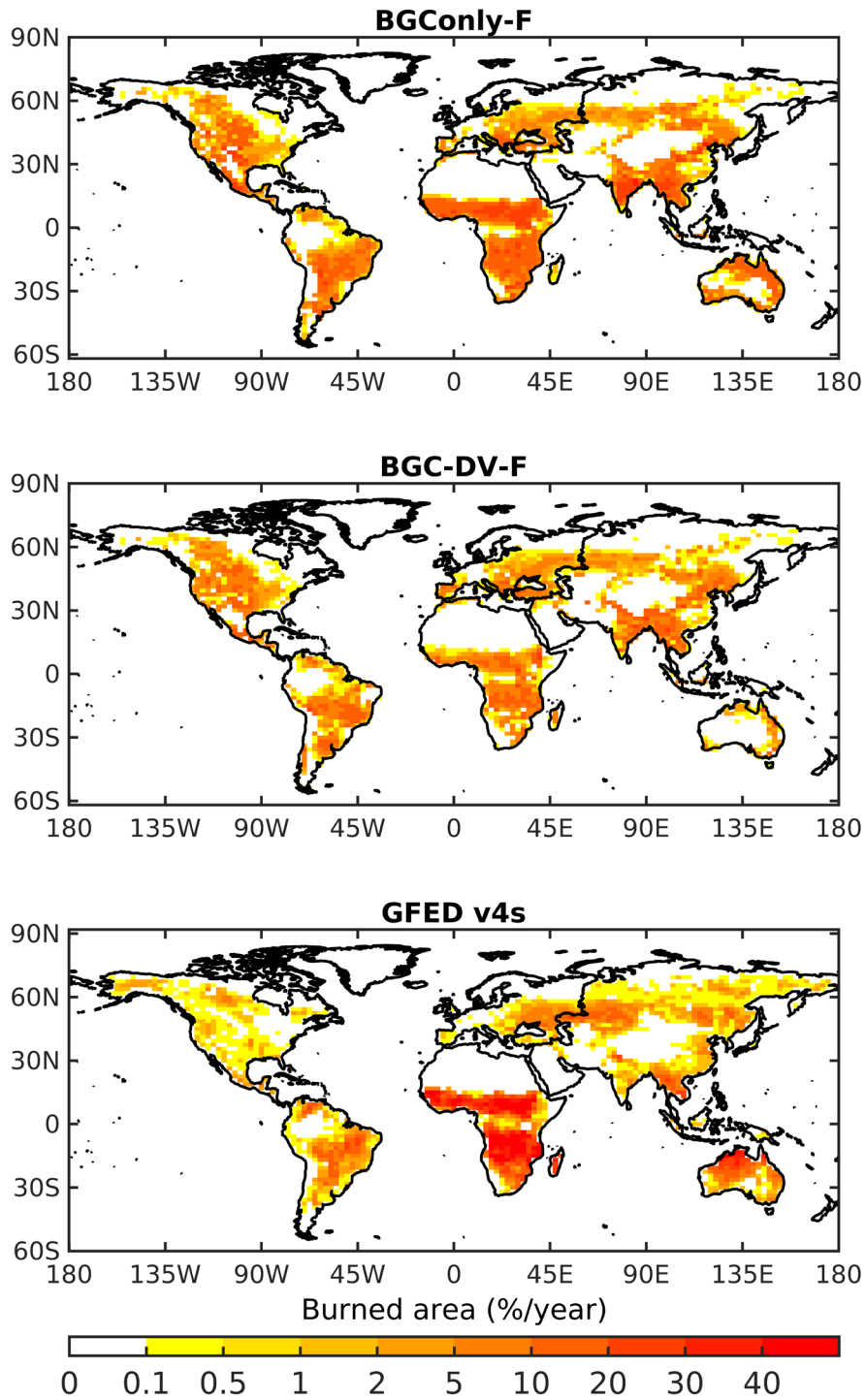
536

537

538 **Figure 2: Annual burned area percentage by grid cell for CLM4.5BGC with fire (BGConly-F), CLM4.5BGCDV with fire**
539 **(BGC-DV-F), and Global Fire Emission Database version 4 with small fires (GFED4s)**

540 .
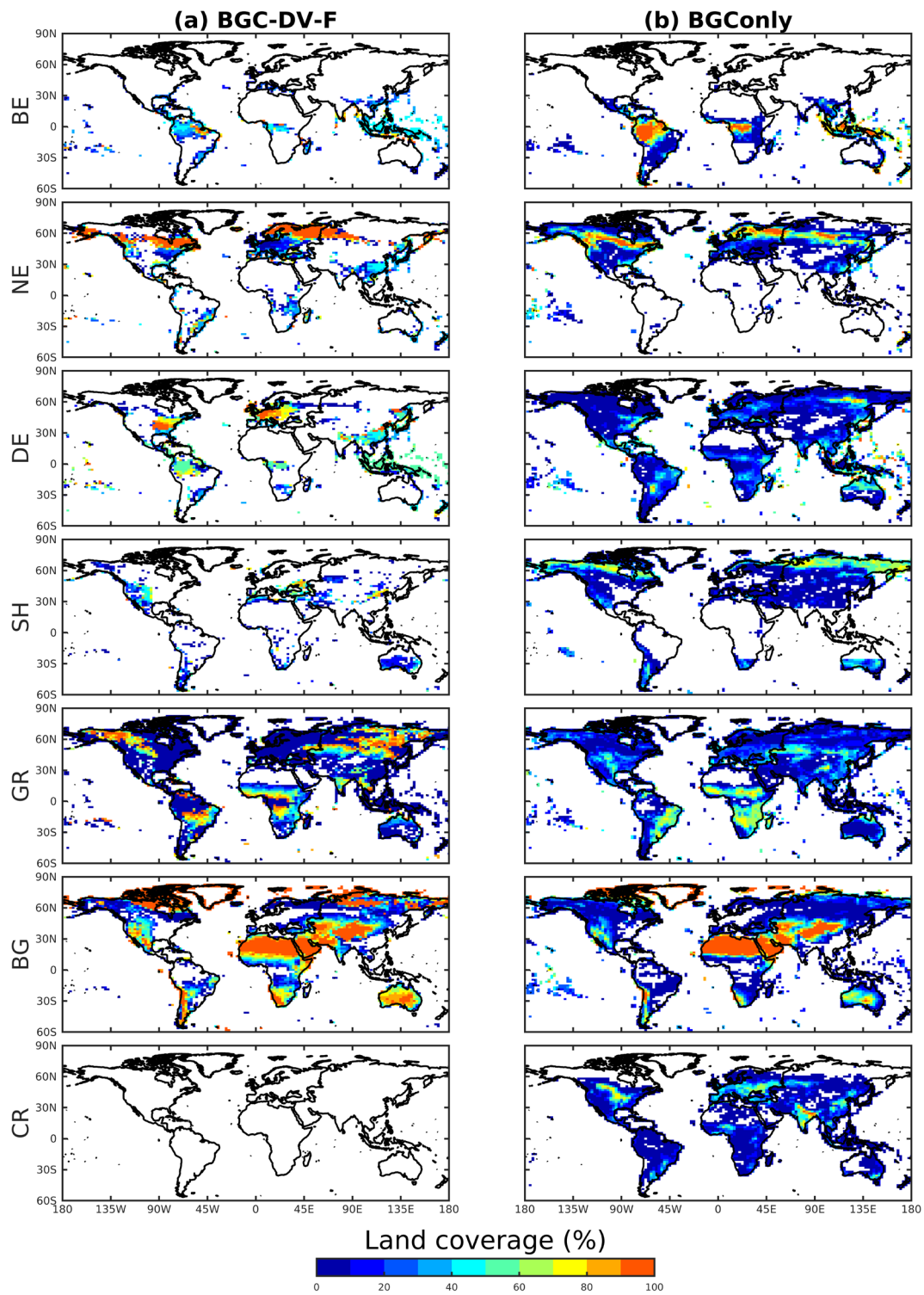
541

542 **Figure 3: Percentages of land cover type (broadleaf evergreen (BE)), needleleaf evergreen (NE), deciduous (DE), shrub**
543 **(SH), grass (GR), bare ground (BG) and crop (CR)) in BGC-DV-F and BGConly (the same for both BGConly-F and**
544 **BGConly-NF).**

545
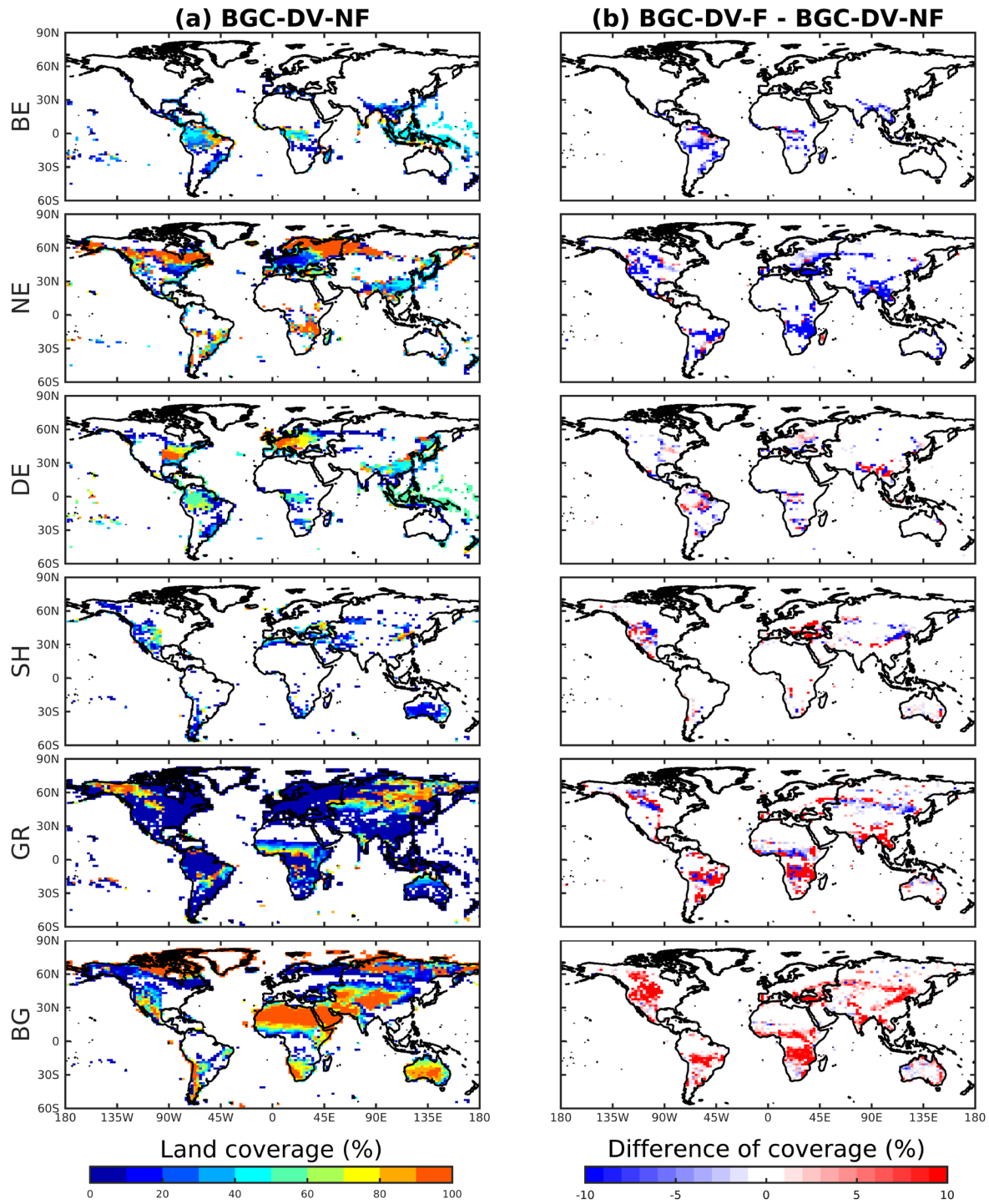
Figure 4: Percentages of land cover (broadleaf evergreen (BE), needleleaf evergreen (NE), deciduous (DE), shrub (SH), grass (GR), and bare ground (BG)) in BGC-DV-NF and differences in plant cover between BGC-DV-F and BGC-DV-NF.

548
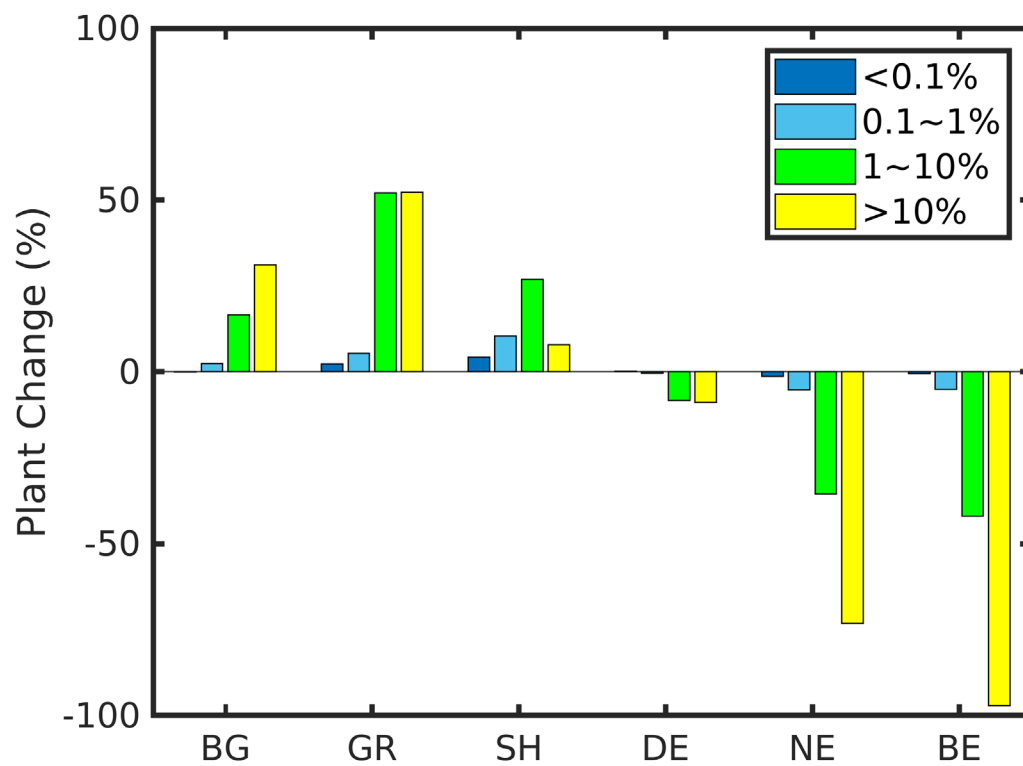
Figure 5: Differences in vegetation distribution (bare ground (BG), grass (GR), shrub (SH), deciduous (DE), broadleaf
evergreen (BE), and needleleaf evergreen (NE)) ratios between BGC-DV-F and BGC-DV-NF for four burned area
categories: under 0.1%, 0.1–1%, 1–10%, and greater than 10%.

552
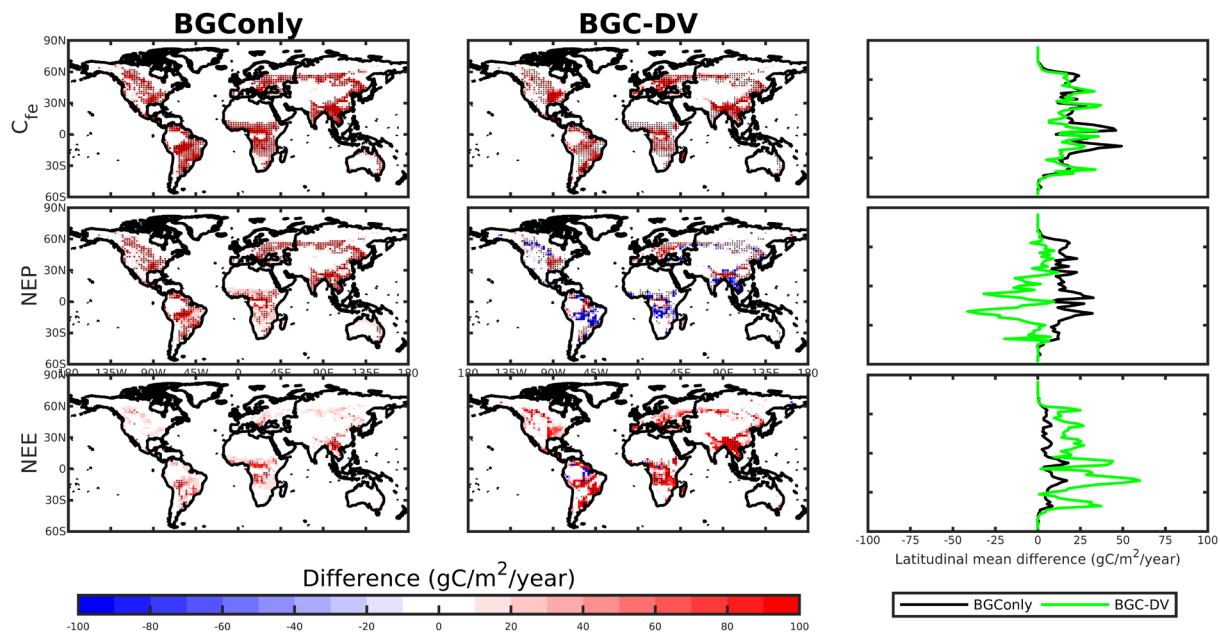
553

554 **Figure 6: Differences in carbon emissions (C$_{fe}$), net ecosystem production (NEP), and net ecosystem exchange (NEE) caused**
555 **by fires in BGConly (BGConly-F minus BGConly-NF; left column) and BGC-DV (BGC-DV-F minus BGC-DV-NF; middle**
556 **column). Hashed areas indicate that the difference passed the Student's t-test at the 0.05 significance level. Latitudinal mean**
557 **differences are plotted in the far-right column.**

558

559

560
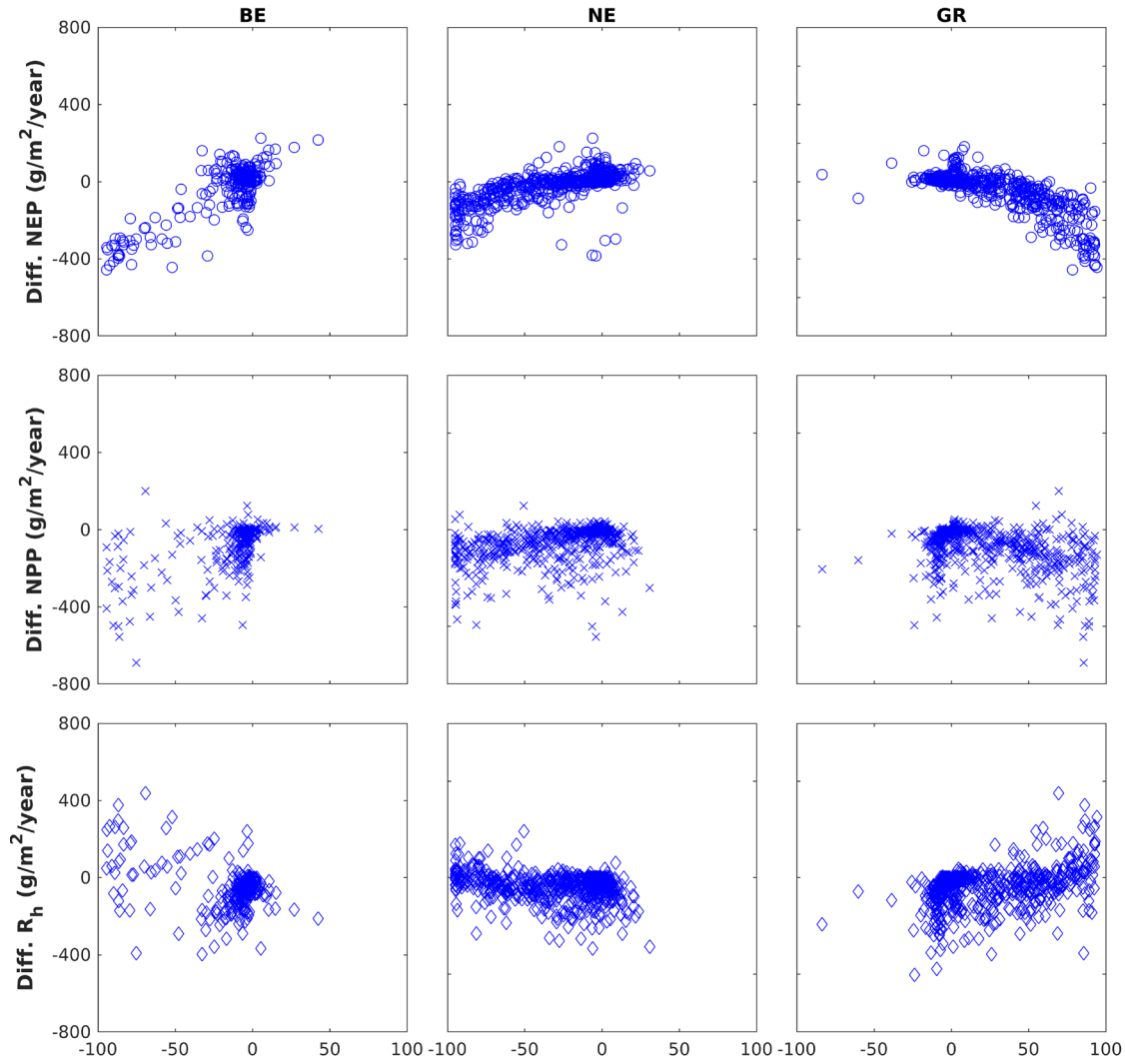
Figure 7: Differences in net ecosystem production (NEP), net primary productivity (NPP), and heterotrophic respiration (Rh)) due to fires in BGC-DV (i.e., BGC-DV-F minus BGC-DV-NF) according to percent changes in broadleaf evergreen (BE), needleleaf evergreen (NE), and grass (GR) vegetation types.

564

565
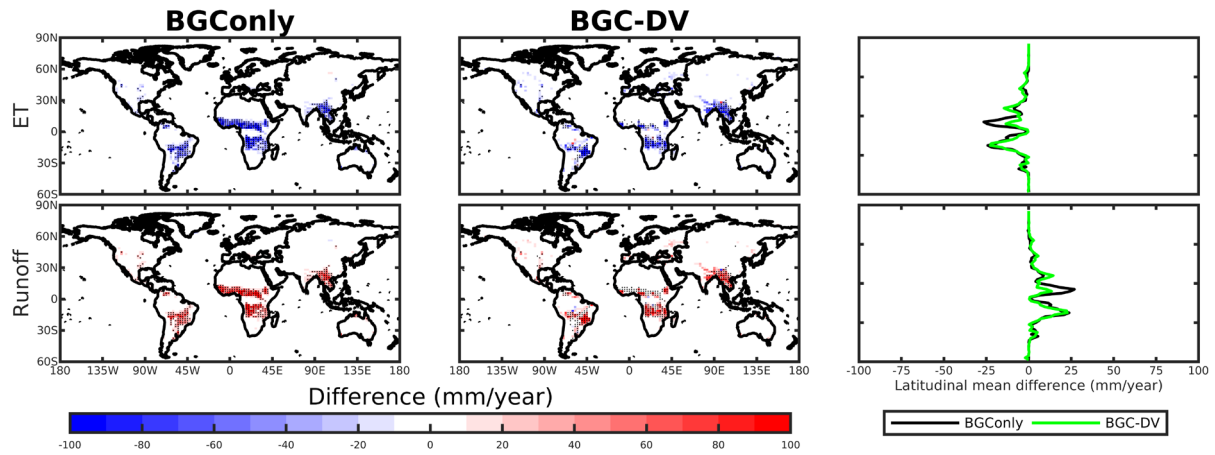
Figure 8: Differences in evapotranspiration (ET) and runoff due to fire in BGConly (BGConly-F minus BGConly-NF; left column) and BGC-DV (BGC-DV-F minus BGC-DV-NF; middle column). Hashed areas indicate that the difference passed the Student's t-test at the 0.05 significance level. Latitudinal mean differences are plotted in the far-right column.

569
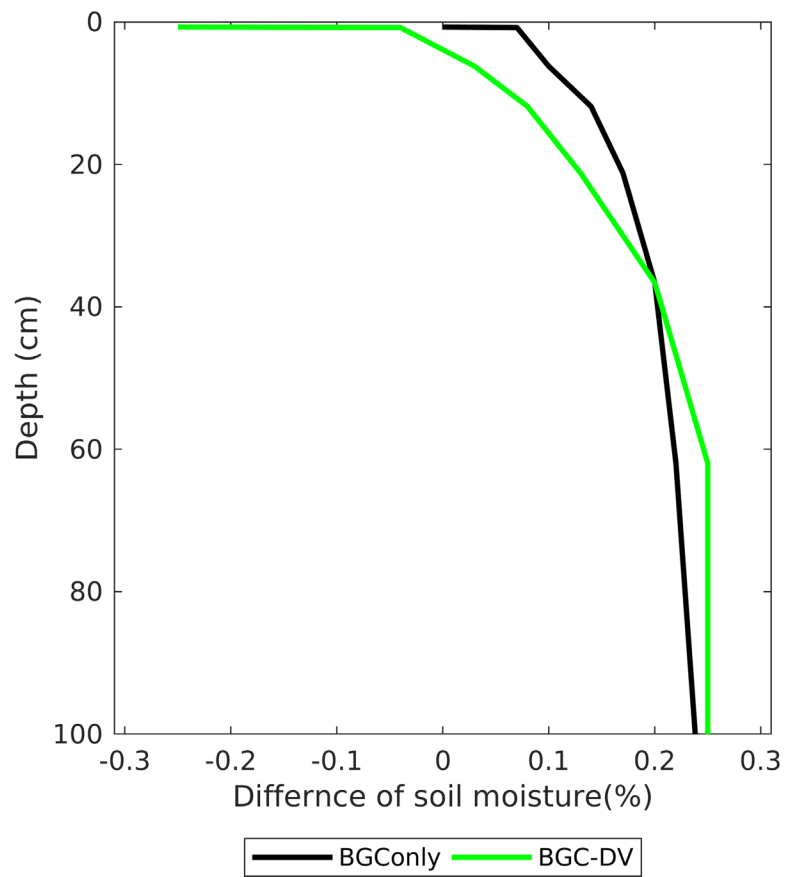
570

571 **Figure 9: Difference in soil moisture (%) due to fire in BGConly (i.e., BGConly-F minus BGConly-NF) and BGC-DV (i.e.,**
572 **BGC-DV-F minus BGC-DV-NF).**

573

     Table 1: Configurations of the experiments used in the study

	BGC for the year 1850	BGC for the 20th century	BGConly	BGC-DV
Time	-	1901–2000	200 yr	200 yr
Climate forcing	Repeated 1901-1920 (CRU-NCEP)	1901–2000 (CRU-NCEP)	Repeated 1961–2000 for five times (CRU-NCEP)	Repeated 1961–2000 for five times (CRU-NCEP)
[CO_2]	[1850]	[1901–2000]	[2000]	[2000]
Biogeography shifts	No	Yes (Prescribed with time-varying PFT distribution)	No	Yes (Simulated in DV mode)
Initial vegetation	No	From BGC year 1850	From BGC for 20th century	No
Initial soil	No	From BGC year 1850	From BGC for 20th century	From BGC for 20th century
PFTs	15 natural + 2 crops for 1850 based on the UNH dataset	15 natural + 2 crops for 20th century based on the UNH dataset	15 natural + 2 crops for 2000 based on satellite data	15 natural (except crops)
Fire	On	On	On (BGConly-F) Off (BGConly-NF)	On (BGC-DV-F) Off (BGC-DV-NF)

576 **Table 2: Percentage (%) land cover types (bare ground, grass, shrub, deciduous, needleleaf evergreen, and broadleaf**
577 **evergreen) in BGConly, BGC-DV-F, and BGC-DV-NF.**

	BGConly	BGC-DV-F	BGC-DV-NF
Bare ground	28.17	41.21	38.66
Grass	20.13	21.25	16.53
Shrub	8.41	4.75	4.24
Deciduous	12.78	12.29	12.67
Needleleaf evergreen	9.96	14.73	20.54
Broadleaf evergreen	10.31	5.73	7.33
Crop	10.25	-	-

578

579

580   **Table 3: Annual means of carbon budget for GPP, NPP, Ra, R_h, NEP, NEE, and C_{fe} and their differences between one with**
581   **fire and one without fire (i.e., BGConly-F minus BGConly-NF, and BGC-DV-F minus BGC-DV-NF) in Pg C yr^{-1}. Asterisk**
582   **(*) index indicates that the difference passed the Student's t test at the $\alpha = 0.05$ significance level.**

	BGConly			BGC-DV		
	BGConly-F	BGConly-NF	Difference	BGC-DV-F	BGC-DV-NF	Difference
C_{fe}	3.49	0.00	3.49*	2.98	0	2.98*
GPP	130.51	144.24	-13.73*	122.01	136.93	-14.92*
NPP	56.66	63.17	-6.51*	52.14	55.56	-3.42*
R_a	73.85	81.08	-7.23*	69.87	81.37	-11.50*
R_h	52.75	61.73	-8.98*	41.19	43.79	-2.60*
NEP	3.91	1.44	2.47*	13.65	14.67	-1.02*
NEE	-0.42	-1.44	1.02*	-5.27	-8.87	3.60*

583

584

585 **Table 4: Pearson correlation coefficients between carbon fluxes (NEP, NPP, R_h) and percentage changes in vegetation cover**
586 **for broadleaf evergreen (BE), needleleaf evergreen (NE), deciduous (DE), shrub (SH), grass (GR), and bare ground (BG).**

	BE	NE	DE	SH	GR	BG
NEP	0.84	0.68	0.34	-0.28	-0.80	-0.14
NPP	0.56	0.44	0.34	-0.30	-0.47	-0.35
R_h	-0.36	-0.17	-0.01	-0.13	0.27	-0.30

587

588

589 **Table 5: Annual mean water budgets for ground evaporation (GE), canopy evaporation (CE), canopy transpiration (CE),**
590 **evapotranspiration (ET), and total runoff (RO) and the difference between the one with fire and the one without fire (i.e.,**
591 **BGConly-F minus BGConly-NF, and BGC-DV-F minus BGC-DV-NF) in 10^3 km^3 yr^{-1}. Asterisk (*) index indicates that the**
592 **difference passed the Student's t test at the α = 0.05 significance level.**

	BGConly			BGC-DV		
	BGConly-F	BGConly-NF	Difference	BGC-DV-F	BGC-DV-NF	Difference
GE	20.87	19.27	1.60*	23.29	19.61	3.68*
CE	15.71	16.39	-0.68*	15.62	16.88	-1.26*
CT	38.41	40.42	-2.01*	37.68	40.99	-3.31*
ET	74.99	76.08	-1.09*	76.59	77.48	-0.89*
RO	31.09	30.02	1.07*	29.51	28.64	0.87*

593

594

595 **Table 6 Annual mean values for LAI (m² m⁻²) and vegetation height (m) and the difference between the one with fire and**
596 **the one without fire (i.e., BGConly-F minus BGConly-NF, and BGC-DV-F minus BGC-DV-NF). Asterisk (*) index indicates**
597 **that the difference passed the Student's t test at the α = 0.05 significance level.**

	BGConly			BGC-DV		
	BGConly-F	BGConly-NF	Difference	BGC-DV-F	BGC-DV-NF	Difference
LAI	2.13	2.36	-0.23*	2.24	2.62	-0.38*
Height	7.05	7.45	-0.4*	6.03	7.76	-1.73*

598

599

600 **Table 7: Annual mean soil moisture (%) at each soil depth and the difference between with fire and without fire cases (i.e.,**
601 **BGConly-F minus BGConly-NF, and BGC-DV-F minus BGC-DV-NF). Asterisk (*) index indicates that the difference**
602 **passed the Student's t test at the α = 0.05 significance level.**

Depth	BGConly			BGC-DV		
	BGConly-F	BGConly-NF	Difference	BGC-DV-F	BGC-DV-NF	Difference
0.71 cm	21.22	21.22	0.00*	20.48	20.73	-0.25*
0.79 cm	23.22	23.15	0.07*	22.59	22.63	-0.04*
6.23 cm	23.24	23.14	0.10*	22.61	22.58	0.03*
11.89 cm	22.72	22.58	0.14*	22.14	22.06	0.08*
21.22 cm	22.37	22.2	0.17*	21.83	21.7	0.13*
36.61 cm	22.48	22.28	0.20*	21.98	21.78	0.2*
61.98 cm	22.57	22.35	0.22*	22.1	21.85	0.25*
103.8 cm	22.45	22.21	0.24*	21.95	21.7	0.25*

603